Research Article/Electrical, Electronic, and Telecommunications Engineering https://doi.org/10.15446/ing.investig.98975

Multi-Tone Optical Source Generation for Applications in Next-Generation Passive Optical Networks using Photonic Structures

Generación de fuentes ópticas multitono para aplicaciones en redes ópticas pasivas de próxima generación usando estructuras fotónicas

Andrés F. Calvo-Salcedo[1], Neil Guerrero-González[2], and José A. Jaramillo-Villegas[3]

ABSTRACT

This study presents the design and simulation of an integrated multi-carrier optical source with a 227 GHz bandwidth for passive optical network (PON) applications. The optical comb generation attained using a photonic structure known as a micro-ring resonator fabricated in silicon nitride (Si3N4) facilitates cost reduction when produced on a large scale. Additionally, the generated optical comb accomplishes non-uniform tones in terms of the optical signal-to-noise ratio (OSNR), which allows for the dynamic assignment of carriers to retainable customers as a function of the data rate and transmission distance requirements. The design and simulation demonstrate the generation of frequency combs with optical carriers in a range of 5-40 tones, an OSNR range of 20-80 dB, and a free spectral range (FSR) of 50-3 610 GHz. To achieve these features, a geometric design of the device is proposed, and its response to variations of input laser parameters is described. In summary, the device uses two optical micro-resonators with radii of 100 and 450 µm and controls the power and the tuning of laser parameters. The proposed method allows generating a deterministic and reliable path to the frequency combs. Finally, the characteristics of the obtained combs are tested to determine their potential use in PON transmissions.

Keywords: next-generation PON, micro-ring resonator, frequency combs, optical communications

RESUMEN

Este trabajo presenta el diseño y simulación de una fuente óptica multiportadora integrada con un ancho de banda de 227 GHz para aplicaciones en redes ópticas pasivas (PON). La generación de peine óptico, que se logra utilizando una estructura fotónica conocida como microresonador óptico fabricada en nitruro de silicio (Si3N4), facilita la reducción de costos cuando se produce a gran escala. Además, el peine óptico generado logra tonos no uniformes en términos de la relación señal óptica a ruido (OSNR), lo que permite la asignación dinámica de portadoras a clientes retenibles en función de los requisitos de velocidad de datos y distancia de transmisión. El diseño y la simulación demuestran la generación de peines de frecuencia con portadoras ópticas con un rango de 5-40 tonos, un rango OSNR de 20-80 dB y un rango espectral libre (FSR) de 50-3 610 GHz. Para lograr estas características, se propone el diseño geométrico del dispositivo y se caracteriza su respuesta ante la variación de los parámetros del láser de entrada. En resumen, el dispositivo utiliza dos microresonadores ópticos con radios de 100 y 450 µm y controla la potencia y la sintonización del láser. El método propuesto permite obtener una ruta determinista y confiable a los peines de frecuencia. Finalmente, se evalúan las características de los peines obtenidos para determinar su potencial uso en las transmisiones con PONs.

Palabras clave: PON de próxima generación, microresonador, peines de frecuencia, comunicaciones ópticas

Received: October 11th, 2021
Accepted: January 19th, 2023

Introduction

A passive optical network (PON) is a fiber network that does not require amplification and power elements to transmit information. This network uses a point-to-multipoint topology and optical splitters to transmit data from a single point to multiple endpoints. In comparison with an active optical network, power is required only at the sending and receiving ends, so this network offers efficiency and low implementation costs (Van Veen, 2020). The growing demand for retainable customers has allowed for the evolution of PONs in recent decades. The advanced modulation formats involved in the process and the use of coherent optical technologies have enabled spectrum optimization and

[1] MSc, Universidad Tecnológica de Pereira, Pereira, Risaralda, Colombia. Affiliation: Professor at Universidad Tecnológica de Pereira, Pereira, Risaralda, Colombia. E-mail: afcalvo@utp.edu.co

[2] PhD, Technical University of Denmark, Lyngby, Denmark. Affiliation: Professor at Universidad Nacional de Colombia, Manizales, Caldas, Colombia. Email: nguerrerog@unal.edu.co

[3] PhD, Purdue University, West Lafayette, IN, USA. Affiliation: Professor at Universidad Tecnológica de Pereira, Pereira, Risaralda, Colombia. E-mail: jjv@utp.edu.co

How to cite: Calvo-Salcedo, A. F., Guerrero-González, N., and Jaramillo-Villegas, J. A. (2023). Multi-Tone Optical Source Generation for Applications in Next-Generation Passive Optical Networks using Photonic Structures. *Ingeniería e Investigación, 43*(2), e98975. https://doi.org/10.15446/ing.investig.98975

increased network speeds (Van Veen, 2020; Serpa *et al*., 2021). Thus, many possibilities for new technology have opened to develop optimization tasks without involving rising costs. Significant advances in photonic devices have enabled the development of integrated circuits for optical digital processing. An example of this is the generation of multi-carrier optical sources, filtering, amplification, and other tasks. These devices help to reduce implementation costs and concurrently optimize the required space, thereby increasing the efficiency of several activities (Van Veen, 2020; Komagata *et al*., 2021). One of the challenges of these networks is the design and implementation of optical sources that allow for the generation of multi-carriers without raising the cost of implementation. One can take advantage of the benefits of transmission methods focusing on wavelength multiplexing transmission by exploring a new issue in parallel transmission and implementing a flexible network (Van Veen, 2020; Serpa *et al*., 2021). This study presents the design and simulation of an optical source based on optical micro-resonators made of silicon nitride. The design of this source offers an approach to a deterministic generation and control of the combs based on the features of geometric rings and power and the tuning of laser parameters. Furthermore, this study presents a strategy to implement a network that allows for spectrum optimization according to distance requirements and the bandwidth of customers, paving the way for the possible creation of next-generation PONs.

The Evolution of PONs

In the 1980s, PONs were identified as an economical and practical method to guarantee broadband to last-mile clients (Serpa *et al*., 2021). In 1995, the full-service access network (FSAN) group formalized a time-division multiplexed passive optical network (TDM-PON) standard. Then, the International Telecommunication Union (ITU-T) standardized two normalized generations of PONs: the asynchronous transfer mode passive optical network (APON) and the broadband passive optical network (BPON). Thus, owing to the importance of the Ethernet protocol, BPONs were modified to allow for frame exchange. Therefore, the Ethernet PON (EPON) standard was created, and a symmetric bit rate was used to upload and download data (FSAN, 2020; Thangappan *et al*., 2020). Subsequently, a standard focused on PON systems of 10 GB, called *XG-PON* (G.987), and EPONs of 10G were introduced. The FSAN group researched 40 Gbit/s PON systems. These systems focused on communication protocols that improved spectral efficiency by highlighting multi-wavelength. This research helped to develop the standard as wavelength-division multiplexing PON (NG-PON2/TWDM-PON – G.989). Although these solutions help with bandwidth implementation, high costs are thereby incurred (Ghoniemy, 2018). The ITU started a process in 2020, attempting to standardize a descending 50 Gbit/s time-division multiplexing-passive optical network (TDM-PON) named *G.hsp*. Recent commercial applications and emergent services such as 5G mobile transport could require symmetric and asymmetric bandwidth in FTTH (Fiber to the Home) applications (IEEE, 2018; Houtsma *et al*., 2021). Currently, the industry is targeting optical access networks focused on wireless traffic, an effort that requires considerable investments in fiber and optic components (Houtsma *et al*., 2021).

Challenges of next-generation PONs

There are multiple challenges in improving bandwidth while reducing costs in optical networks. Factors such as equalization, error correction, energy optimization, flexible design, and low-cost source design should be considered. Next-generation PONs should flexibly connect to networks. In addition, the characteristics of point-to-multipoint communications established in standardized PONs demonstrate the advantage of a flexible line rate. This flexibility enables wideband reconfiguration, transmission speed, and cost based on customer demand. Because of this, it is necessary to develop new approaches capable of optimizing network flexibility by taking advantage of optical comb generation, power supply, and the separation of end users (Houtsma *et al*., 2021; Shbair *et al*., 2021; Rodríguez-García *et al*., 2021). Electronic and photonic integration will be an issue of next-generation PON design.

Reducing costs in multitone generation is a significant issue. The incorporation of a wavelength involves the addition of a laser, which increases the investment costs. However, this device constrains the number of tones for transmission and reception. Increasing the number of wavelengths or reducing the required lasers can make this technology more attractive to last-mile customers. Hence, implementing these methods could increase the speed of transmission. Consequently, the photonic approach becomes a focus for improving the design of PONs. This approach makes it possible to create portable devices that generate multitone while using only one laser. These devices are known as *micro-ring resonators* and enable the application of this technology due to the generation of frequency combs (Lundberg *et al*., 2020). Frequency combs refer to a set of evenly spaced spectral lines that are well-defined in the frequency spectrum. This concept allows using every tone to generate PON transmission in an ascending or descending manner (Lundberg *et al*., 2020).

Frequency comb generation: applicability in photonic integration

Recent studies have accomplished frequency combs for coherent optical communication systems. Transmission speeds –including 1,44Tbit/s– have been attained in distances close to 80km using up to 25 tones. Although these methods generate a multitone source to be applied in advanced modulation techniques, they are made with electro-optical elements, ignoring the features of frequency combs manufactured with photonic integrated optical micro-resonators. A frequency comb generates numerous wavelengths with equally separated frequency and phase synchronization. Its generation depends on a double balance between loss and input power, as well as on nonlinearity and Kerr's dispersion (Kippenberg *et al*., 2020). In addition,

different techniques have been implemented for generating frequency combs, which enables the appearance of multiple frequency components in the generated signal.

A common technique is a cascade of optical modulators, which harnesses the benefit of the spread spectrum via phase and amplitude modulation to make new tones in the spectrum from a nonlinear process. Although this technique generates frequency combs, it usually has a high insertion loss (6dB). It also requires large dimensions to reach integration (centimeter scale), which is a disadvantage for implementing this technique in optical networks. The typical component used in this application is lithium niobate ($LiNbO_3$). Other methods use modulators with indium phosphide (InP) semiconductors, where the dimension reduction is considerable and the insertion loss is still high (5dB) (Komagata *et al.*, 2021). Applying recirculating ring modulators is another technique used for optical combs generation. This method uses the recirculation of the wavelength through a phase modulator supplied by a radio-frequency oscillator. Thus, sidebands around the leading tone are generated. Moreover, when the output recirculation is executed, new sidebands are generated around the others, developing a frequency comb. Although this technique manages to yield a spread bandwidth (1THz), it requires a large dimension (meters) to configure the recirculating structure (Mittal *et al.*, 2021).

A different approach involves using a continuous wave laser and modifying its power, detuning in a resonance frequency and thus generating an optical frequency comb (Kippenberg *et al.*, 2020; Mittal *et al.*, 2021). This technique has advantages in frequency comb stability and the noise made. On the other hand, its integration is reached in lithography by using materials such as SI_3N_4 and SiO_2, and it does not require large dimensions (Kippenberg *et al.*, 2020). Although using a pulsed laser has advantages on frequency combs generation, it requires modifying input parameters for laser power and frequency detuning. Depending on the input conditions, it is possible to attain different performance behaviors on the cavity.

These behaviors generate different spectral response patterns, such as stable cavity solitons (SCS), unstable cavity solitons (UCS), and stable modulation instability (SMI-Turing rolls) (Kippenberg *et al.*, 2020; Komagata *et al.*, 2021; Jaramillo-Villegas *et al.*, 2015; Qi *et al.*, 2019). In the spectral domain, these patterns generate optical frequency combs with multitone. Turing rolls are one of the most interesting patterns for generating optical sources (Qi *et al.*, 2019). This approach involves several oscillating pulses throughout the azimuthal direction in the disc and generates an optical frequency comb in its spectrum, with stabilization of the free spectral range (FSR). This comb is considered to aid optical communications because it is more effective against noise. Moreover, it provides consistency within individual comb lines and brings more stability to maintain the pattern over time (Qi *et al.*, 2019). One key to this frequency combs generation is avoiding the chaotic region. Turing rolls provide a solution because they generate combs to keep the power laser constant by applying the linearly swept frequency theory. Other patterns such as SCS or UCS require specific controllers to achieve exponential functions in laser power variation. This increases implementation costs and prevents the use of SCS and UCS combs (Mittal *et al.*, 2021). Many researchers support using compound-ring resonators and thermal control to easily modify the device dynamics and access regions in the parametric space (Ma *et al.*, 2021; Jaramillo-Villegas *et al.*, 2015; Chaitanya *et al.*, 2016; Xiaobao *et al.*, 2021). Although these techniques enable the study of SCS and UCS regions, the generation of frequency combs depends on complex controls involving nonlinear pathways.

Other approaches use optical micro-resonators and Mach-Zehnder modulators, which allow generating a flat comb with numerous wavelengths. Although researchers have achieved high-speed transmissions, these approaches increase the economic costs of implementation by requiring additional processing and not using the optical comb generated by the micro-resonator alone (Das, 2020; Dutta, 2022). Recently, it was possible to demonstrate a transmission of 1,84 Pbit/s over a 37-core, 7,9 km-long fiber via 223 wavelength channels using optical micro-resonators. Although this approach showed the potential for this type of application, its goal was communication with a single receiving transmitter and the maximization of the speed that can be achieved, meaning that a PON scenario was not considered (Jørgensen, 2022). This research proposes a novel approach for generating frequency combs in PON optical communications through the use of micro-resonators as multi-tone sources. A reliable route has been developed based on the intrinsic parameters of the micro-resonator structure, demonstrating the feasibility of this technique for frequency combs generation in PONs.

Methodology for optical frequency combs generation

This research adopts a three-stage methodology (Figure 1) in a PON to generate a comb. First, the design of an optical micro-resonator structure that aims to define an adjusted geometry to a dynamic response or resonator is considered. Second, the parametric space is characterized as $(\Delta, |S|^2)$ in order to understand how these parameters are involved in comb generation. Thereupon, these different approaches enabling frequency combs generation on Turing rolls and USC regions are suggested (Qi *et al.*, 2019). Lastly, the generated comb is tested to verify whether it meets the spectral features to function as a multitone generation source.

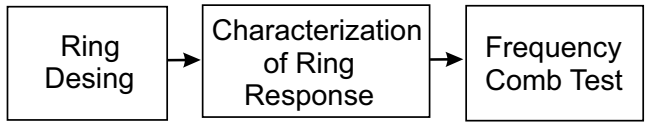

Figure 1. Methodology diagram
Source: Authors

To design a photonic device for multi-carrier generation, a proposed MRR is presented in Figure 2. The selected waveguide and cladding materials are Si_3N_4 and SiO_2, respectively. This structure exhibits an anomalous dispersion with a quality factor $Q = 1,67\times10^6$ and photon lifetime $t_{ph} = t_R/(2\alpha) = 1,37\,\text{ns}$. It is necessary to differentiate the FSR from frequency combs, so this study recommends using two different radius values (100 and 450μm). These values generate FSR 227 and 50GHz. Hence, two different FSR are considered to fulfill different customer bandwidth requirements. This physical configuration is selected because large dimensions (μm) are not required, and those FSR values allow for bandwidths suitable for communications applications. The Lugiato-Lefever Equation (LLE) is used to simulate the optical combs generation process in the micro-resonator structure, as well as split-step Fourier as a solution method (Jaramillo-Villegas *et al.*, 2015). This approach allows verifying the dynamic response of the ring and its spectrum when different variations of input laser parameters are generated. The following simulation parameters are used in the first ring: $t_R = 1/226\,\text{GHz}$, $\beta_2 = -4,7\times10^{-26}\,\text{s}^2\text{m}^{-1}$, $\alpha = 0,00161$, $\gamma = 1,09\,\text{W}^{-1}\text{m}^{-1}$, $L = 2\pi\times100\,\mu\text{m}$, and $\theta = 0,00064$ (Chaitanya *et al.*, 2016; Xiaobao *et al.*, 2021). The following simulation parameters are used in the second ring: $t_R = 1/50\,\text{GHz}$, $\beta_2 = -4.7\times10^{-26}\,\text{s}^2\text{m}^{-1}$, $\alpha = 0,00161$, $\gamma = 1,09\,\text{W}^{-1}\text{m}^{-1}$, $L = 2\pi\times450\,\mu\text{m}$, and $\theta = 0,00064$ (Chaitanya *et al.*, 2016; Xiaobao *et al.*, 2021).

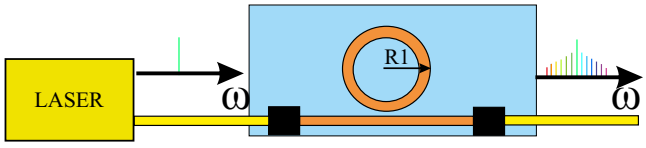

Figure 2. Micro-ring resonator structure for frequency combs generation
Source: Authors

Anomalous dispersion is used in the simulation. Moreover, simulations are performed to initialize the intra-cavity field in the frequency domain E(ω) with a circularly symmetric complex Gaussian noise field with a standard deviation $10^{-9} = 10^{-9}$ [$P = |E|^2$]. In addition, the normalization $P = |E|^2$ is equivalent to a mean power of -150 dBm per cavity mode and a random uniform phase that aims to create a realistic condition. To obtain the parametric space $(\Delta, |S|^2)$, the power and the detuning of input laser are swept. First, indicating the starting point $(\Delta_1, |S_1|^2)$, a path with a linear sweep to a final point is generated $(\Delta_2, |S_2|^2)$. The next step is counting the number of pulses produced in a round-trip, and each region is characterized depending on the number of peaks (Jaramillo-Villegas *et al.*, 2015). These results are shown in Figures 3b and 3e. If the signal behavior shows fewer peaks, its FSR will be smaller. By contrast, if the signal behavior has more peaks, its FSR increases. In Figures 3b and 3e, parametric spaces for the suggested method are shown. In Figure 3c, SCS and USC regions appear in the upper right corner of the graph. These regions cannot be attained with a constant power parameter. Hence, this generation is difficult due to the exponential power variation required to avoid the chaotic region. However, Figure 3c shows that the SMI-Turing rolls region is on the left side of the graph, making it accessible to create a path with power constantly avoiding the chaotic region and enabling combs generation (Figures 3b and 3e). The magenta hexagon indicates the initial point where characterization and simulation start. This point is chosen due to its stability and low-intensity noise. However, the Turing rolls achieve phase-locked states that are independent of the initial conditions (Jaramillo-Villegas *et al.*, 2015).

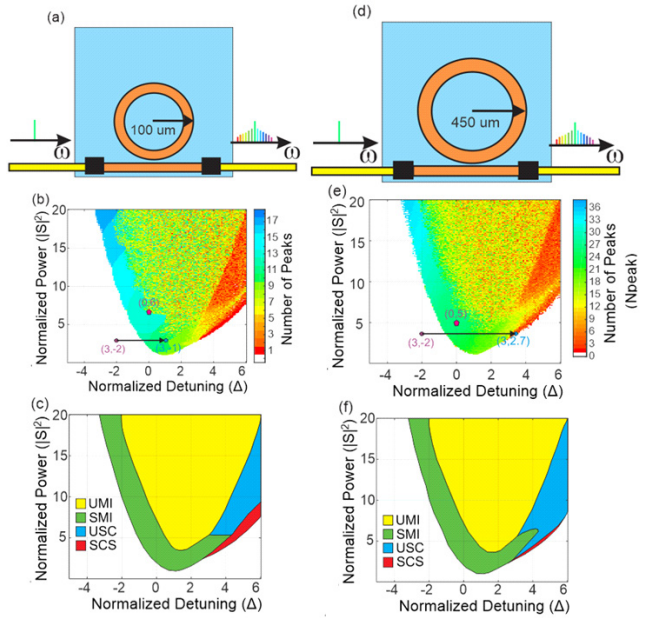

Figure 3. a) Basic structure of an MRR with an FSR of 226 GHZ . **b)** Parametric spacing as a function of the number of peaks $(\Delta, |S|^2)$ with respect to the MRR with an FSR of 226 GHZ. **c)** Characterization of regions according to variation $(\Delta, |S|^2)$ regarding the MRR with an FSR of 226 GHZ. **d)** Basic structure of an MRR with an FSR of 50 GHZ. **e)** Parametric space as a function of peak numbers $(\Delta, |S|^2)$regarding the MRR with an FSR of 50 GHZ. **f)** Characterization of regions according to variation $(\Delta, |S|^2)$regarding the MRR with an FSR of 50 GHZ.
Source: Authors

The optical frequency combs can be generated by decreasing the optical frequency of the pump laser towards the resonance, which makes this pattern a good choice for the initial point. To demonstrate the combs generation, several paths to the SMI region are proposed.

This region was selected because optical frequency combs of the Turing rolls type are robust to noise and exhibit high coherence among the individual comb lines. At the same time, it is possible to ensure a trajectory with constant power to control input variables. This simplifies the generation process by creating a path that only requires linear variation of the frequency.

A path with a constant power that has been normalized is defined. Subsequently, a linear tuning sweep that has also been normalized is performed along this path. An adiabatic process is considered for manipulating the laser input parameters because the variation must be slow. This, in order to ensure processing in the computational systems. Accordingly, the total simulation time is 1 ms.

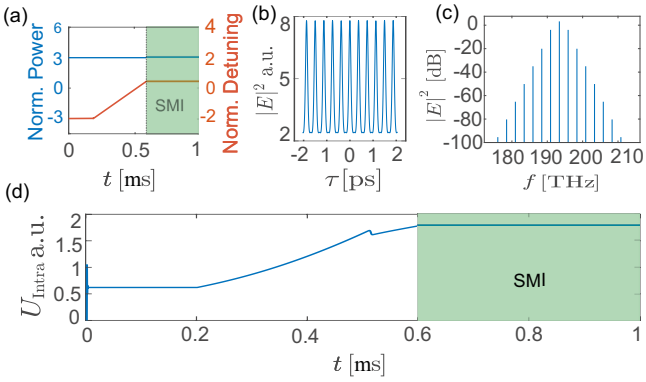

Figure 4. a) Power pump (blue) and detuning (red) in a slow time (t). **b)** Intensity value. **c)** Spectrum. **d)** Intracavity energy against time (t) to reach the point of Figure 5a.
Source: Authors

Figures 4 and 5 show the suggested paths to frequency combs generation based on the characterization shown in Figures 3b and 3e.

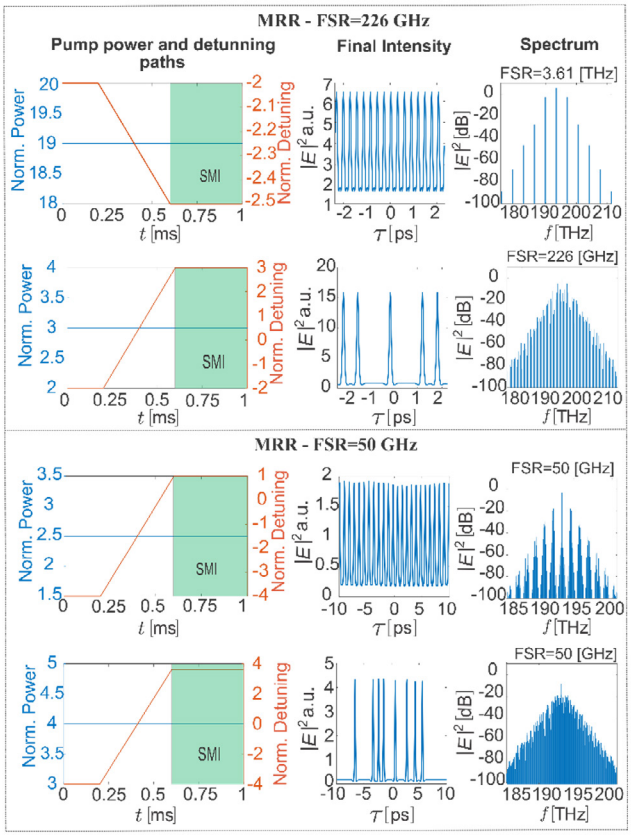

Figure 5. Results of the simulation regarding frequency combs generation
Source: Authors

According to Figure 5, different frequency combs are ensured depending on the power and tuning values. In contrast, peak numbers are lower where the FSR decreases in the intensity graph. Hence, it is important to highlight the line separation change depending on the ring ratio, as well as the result with 36 peaks for the structure with a radius of $450\,\mu m$, achieving an FSR smaller than a comb of $100\,\mu m$ peaks with a $100\,\mu m$ ratio. The combs obtained in this work do not have noise because they are the results of a simulation. This factor is important because the wavelengths of the comb have higher ONSR than those generated in a real device. To avoid this problem, the spectral power of each wavelength is reduced, since this would be the effect that produces noise in the photonic structure.

It is important to emphasize that each ring has different features depending on its geometry, and it attains different FSR and different bandwidths. The frequency comb test calculates the behavior of the total intracavity power for a comb of 16 peaks. This parameter is used because it is proportional to the integral result of intensity during a round trip, enabling the generation of an idea of comb stability. In Figure 5d, the micro-resonator exhibits stable generation as it does not generate oscillatory behaviors when located within the SMI region. This observation underscores the robustness and reliability of the micro-resonator in generating stable signals. This behavior allows deducing permanence, one of the main features of using it as an optical source.

Application of frequency combs to next-generation PONs

The application of optical frequency combs focuses on long-distance communication networks with a fixed transmission distance. This implies that device design methods attempt to achieve many spectral lines with the minimum possible power, generating a spectrum with uniform carriers. Some optical processing activities that spend more energy must be executed in order to fulfill this task. Furthermore, wavelengths are discarded because they do not perform the activities with the required power levels. Hence, limiting the carrier numbers and spending significant resources on other scenarios must be considered (Van Veen, 2020; ITU, 2021). However, the PON scenario is different because its approach is multi-point. These networks focus on the last-mile customer, and the distances change from the central node –distances close to 80 km are also considered. Consequently, a frequency comb with different energy levels is desirable as a multi-carrier source.

This has two significant advantages. First, optical micro-resonators are used because they generate a comb with carriers and different energy values. Second, any activity that attempts uniformity in a comb is avoided, decreasing the implementation costs of the network. There is another issue for consideration in this case: the optical signal-to-noise ratio (OSRN) directly combines two essential features of the network. First, when the OSNR increases, the transmission distance becomes larger since the information is acquired quickly. Second, when the OSNR increases, it is possible to increase the modulation order, optimizing the spectral efficiency. The algorithm must assign spectral lines suitable for bandwidth and distance demand. Wavelength numbers and energy values specific to the frequency comb must be established. Furthermore, this approach must create a modulation format that sends information via wavelength-division multiplexing (WDM) according to the OSNR features.

Figures 6a and 6b illustrate the significance of increasing the OSNR as the transmission distance growing. Therefore, the farthest customers use the blue carriers. Orange-colored customers use spectral lines with less energy than blue ones. Finally, green customers use tones with less energy, allowing them to assign spectral lines according to distance requirements. In Figure 6, a graph presents two scenarios with PONs. The first scenario shows a network with three customers located at different distances. In Figure 6d and 6e, one customer requires significant bandwidth. The second scenario adds different bandwidths in the same network.

These scenarios show how to use frequency combs according to OSNR, distance, and bandwidth. Hence, when multiple carriers are implemented, communication protocols can be applied for multi-wavelengths to take advantage of the spectrum. In contrast, the green customer requires a BW2 bandwidth, implying fewer spectral wavelengths. In this case, lines with more energy are assigned according to the customer's distance. The scenarios in Figure 6 help to verify the number of carriers of frequency combs to optimize the current spectral resources. This aids in cost reduction and optimizes the optical source. These traits allow this method to set these types of sources in next-generation PON design.

To verify the use of optical combs, a test is proposed in which different request scenarios are simulated in an optical network. The network consists of multiple users and an optical micro-resonator source. This network uses wavelength multiplexing and transmits the signals using 16 QAM modulation, with a BER = 0,7 x 10^{-9} and an attenuation for the waveguides of 0,2 dB km^{-1}.

The ONSR of each wavelength is also decreased by 50 dB to simulate the noise conditions of a real device. A wavelength allocation algorithm was designed with this scenario, based on the abovementioned rules. This algorithm uses information from the frequency comb, such as the number of carriers, the OSNR, and the modulation format, in order to calculate the transmission distances that each carrier can guarantee without compromising the quality of service (QoS).

Our assignment algorithm searches for available wavelengths in the optical source and computes the maximum transmission distance of each wavelength for the 16 QAM modulation format. Subsequently, calculating the required number of carriers for each request, the wavelengths are assigned, ensuring that they have a greater distance than what is requested by the customers' location. This algorithm prioritizes requests with greater distance due to the physical shape of the comb.

Otherwise, the wavelength with the longest transmission distance could be assigned to a request very close to the central office, thus wasting resources. Therefore, the requests are organized from longest to shortest distance, and from highest to lowest bandwidth. The allocation algorithm is presented in Figure 7.

Initially, the allocation process is visualized, proposing an optical frequency comb with 11 lines and an FSR of 50 GHz. In parallel, a scenario with four clients with different bandwidths is offered, and the allocation process involving the proposed algorithm is observed. Here, the first user requests 400 Gbit/s at 25 km, the second user requests 100 Gbit/s at 70 km, the third user requests 300 Gbit/s at 40 km, and the fourth user requests 70 Gbit/s at 40 km.

Figure 8 shows the 11 lines of the optical comb, their kilometer capacity, and the spectrum allocation result for the four requests. Note that our method assigns the request of the second customer to the wavelength with the highest distance capacity, and it assigns the other requests according

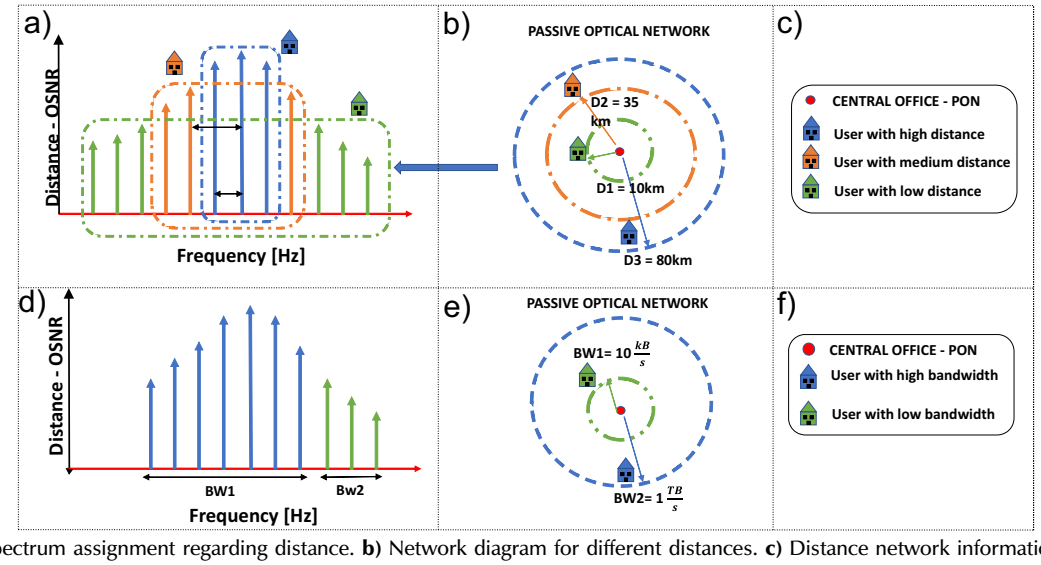

Figure 6. a) Spectrum assignment regarding distance. **b)** Network diagram for different distances. **c)** Distance network information. **d)** Spectrum assignment regarding bandwidth. **e)** Network diagram for different bandwidths. **f)** Bandwidth network information.
Source: Authors

to the distance required by each demand. Also note how the requests with bandwidths of 400 and 300 Gbit/s use super-channels to support the modulation. The above allows verifying that the algorithm responds to the ideas put forward for the allocation.

```
input:
atf     % Fiber attenuation dB/km
BER     % BER of communication
FSR     % Free spectral range
Bd[j]   % Bandwidth of the jth client
Dd[j]   % Distance of the jth client
P44     % Comb spectrum dB
EbEN0   % OSNR for BER and 16QAM modulation
tamd    % Requests size
tams    % Slot size
Ouput:
VA      % Accepted assignment array
RE      % Rejected requests array
%% Computation of bandwidth for 16 QAM modulation and
wavelengths
for j=1:length(dd)
 bw_mod[j]=compute_BW(Bd[j],'16QAM');
 num_WL[j]= number_wavelengths(FSR,bw_mod[j]);
end
dist=(fre_comb-EbEN0)./atf;
% Calculate requests by distance and bandwidth
VP=0.2*Bd+0.8*dd;
% Sort by bandwidth and distance based on VP [bd1,dd1, num_
WL1]=sort(VP,Bd,Dd);
D2=dist;
%% Allocation process
VA=zeros(1,tams);
for i=1:length(bd1)
  r=D2>=dd1[i];
  if sum(r)>= num_WL1[i]
   % Find the consecutive wavelengths
   cell=separate_consecutive(r);
   % Compute group sizes
   tcel=length(cell)
   for j=1:tcel
   CE=cell{j};
   % Select candidate group
   if length(CE)>= num_WL1[i]
    jj=jj+1;
    for K=1:num_WL1[i]
    % Index VA with the request identifier
    VA[CE[K]]=ibd[i];
    % Fill in the assigned wavelengths with zeros
    D2[CE(K)]=0;
    end
% Stop iteration when ibd[i] is allocated
    break
   end
  end
 end
 if jj==0
   % Store rejected demand with ibd[i] value
   con=con+1;
   RE[con]=ibd[i];
 end
end
```

Figure 7. Allocation algorithm
Source: Authors

Initially, the allocation process is visualized, proposing an optical frequency comb with 11 lines and an FSR of 50 GHz. In parallel, a scenario with four clients with different bandwidths is offered, and the allocation process involving the proposed algorithm is observed. Here, the first user requests 400 Gbit/s at 25 km, the second user requests 100 Gbit/s at 70 km, the third user requests 300 Gbit/s at 40 km, and the fourth user requests 70 Gbit/s at 40 km.

Figure 8 shows the 11 lines of the optical comb, their kilometer capacity, and the spectrum allocation result for the four requests. Note that our method assigns the request of the second customer to the wavelength with the highest distance capacity, and it assigns the other requests according to the distance required by each demand. Also note how the requests with bandwidths of 400 and 300 Gbit/s use super-channels to support the modulation. The above allows verifying that the algorithm responds to the ideas put forward for the allocation.

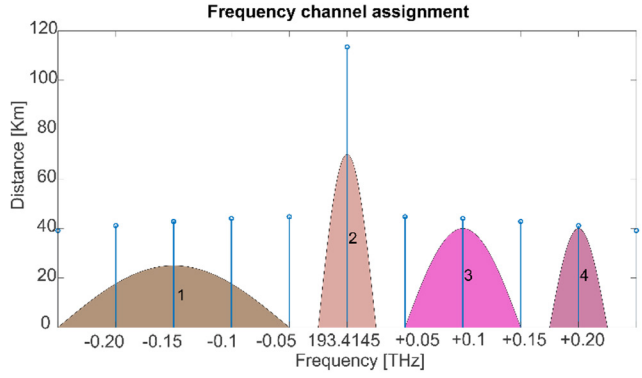

Figure 8. Spectrum allocation
Source: Authors

Next, a network scenario is created in which different request configurations are proposed and the allocation algorithm is computed to verify the network bandwidth blocking ratio in 200 scenarios. To simulate each scenario, our experiment models the number of users, their bandwidth, and their distances to the central office as discrete random variables.

This ensures that each request has the same probability of appearing. The range of users varies between [1 100] users, the bandwidth varies between [1 100] Gbit/s, and the distances are between [0 and 80] km.

Figure 9 shows the algorithm responsible for the 200 scenarios. For each of these, the bandwidth blocking ratio is computed $\left(BBR=\frac{\sum_{i=1}^{n} BWR_i}{\sum_{i=1}^{n} BWS_i}\right)$ because it allows quantifying how much bandwidth can be allocated in a set of requests. Note that our proposal obtains 99 requests with zero blocking probability (Figure 10). This is because our method uses wavelengths that were discarded for having low spectral power in other approaches.

The results above show the potential of the proposal; note that, when the bandwidth and the number of customers grow to high values, the comb cannot support the requests

(Figure 9). This implies that optical combs must be generated with as many lines as possible in order to extend the capacity of the proposal.

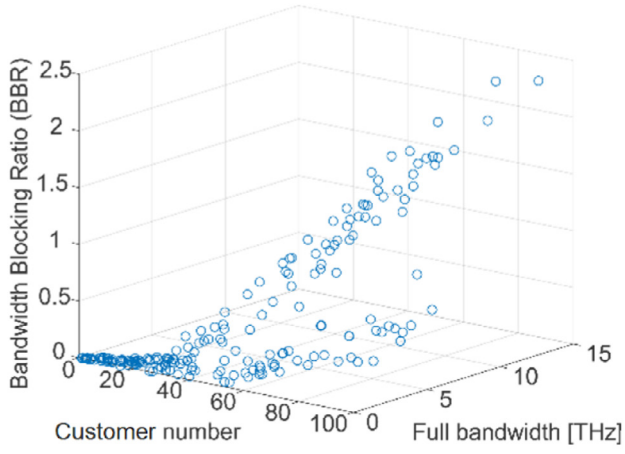

Figure 9. Customer number and full bandwidth *vs.* bandwidth
Source: Authors

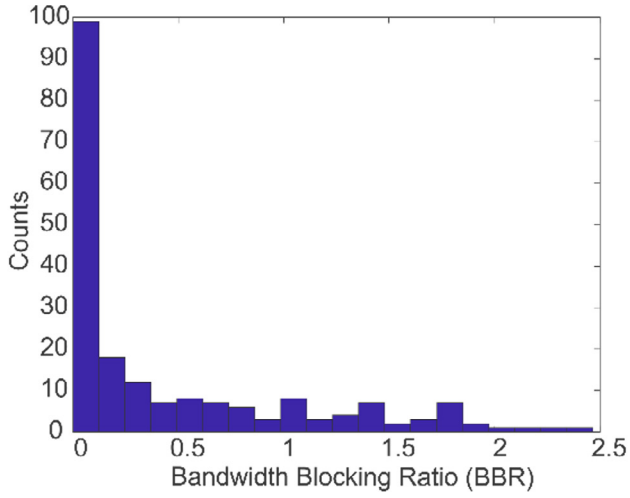

Figure 10. BBR histogram for 200 repetitions
Source: Authors

Conclusions

This paper presents a significant vision for the development of next-generation passive optical networks (PONs). First, it discusses the concept of flexibility, in which an optical network generates adaptive solutions while considering the fluctuation of bandwidth demand and its increasing trend. The method provides multiple carriers with a different signal-to-noise ratio (SNR), which allows assigning wavelengths according to the distance requirements of the customers' geographic locations. This solution optimizes the energy consumption of network resources. To accomplish these goals, modulation formats with high spectral efficiency must be used, which requires using coherent technology to perform phase and amplitude modulation, including multiplexing approaches such as wavelength-division multiplexing (WDM), which allow for the parallel transmission of multiple wavelengths and facilitate the transmission of information. Thus, an optical source is designed to generate multiple wavelengths while using only one laser. This optimizes the implementation costs because it avoids buying numerous sources. To this effect, optical micro-ring resonators are used. These rings should be designed in silicon nitride (Si_3N_4) to take advantage of its photonic integration. Their design must be replicated in an optical chip that requires little space, allowing to replicate it on a large scale and reduce energy consumption. Hence, by applying this technology, costs are reduced. To obtain a robust optical source that guarantees transmission, the laser parameters are controlled to achieve a frequency comb in the Turing rolls and SCS regions. These regions are selected because they feature spectral sources that are constant without considering wastage issues and waveguide dispersion. Moreover, the control algorithm is easily replicated with current network devices. This is because it does not require varying the laser power, and frequency tuning is performed with a linear sweep. The reliability of this approach allows differentiating the FSR of the comb, achieving the different bandwidths used in the flexible scenario. A physical device could be designed in future works which enables the generation of multiple carriers, digital processing techniques, and machine learning, allowing for the dynamic assignation of wavelengths according to the customer's bandwidth requirements and distance. To this effect, two criteria must be applied. The first one depends on the optical SNR of carriers with the distances of the end users; when the SNR increases, it should attain more distance. The second criterion is the bandwidth requirement, as a high number of carriers will be assigned, or the spectral distance will be modified to increase or decrease the bandwidth. This will enable the development of new future telecommunication services that help society in terms of production, economics, and the development of new technologies. This, including the least developed countries, where the development of telecommunications is essential.

Acknowledgements

The authors would like to thank Universidad Tecnológica de Pereira and their support from the program titled *Reconstrucción del tejido social en zonas de posconflicto en Colombia*, part of the Project *Modelo ecosistémico de mejoramiento rural y construcción de paz*, funded by Fondo Nacional de Financiamiento para la Ciencia, la Tecnología y la Innovación, Fondo Francisco José de Caldas (contract no. 213-2018, code 58960).

CRediT author statement

All authors: Conceptualization, methodology, validation, formal analysis, investigation, writing (original draft preparation, review, and editing), data curation, supervision, project administration, resources, and funding acquisition.

References

Chaitanya, J., Jae K. J., Luke, Kevin., Xingchen J. I., Miller, S. A., Klenner, Alexander., Okawachi, Y., Lipson, M., and Gaeta, A. L. (2016). Thermally controlled comb generation and soliton modelocking in microresonators. *Optics Letters, 41*(11), 2565-2568. https://doi.org/10.1364/OL.41.002565

Das, B., Mallick, K., Mandal, P., Dutta, B., Barman, C., and Patra, A. S. (2020). Flat optical frequency comb generation employing cascaded dual-drive mach-zehnder modulators. *Results in Physics, 17*, 103152. http://doi.org/10.1016/j.rinp.2020.103152

Dutta, B., Sarkar, N., Atta, R., Kuiri, B., Santra, S., and Patra, A. S. (2022). 640 Gbps FSO data transmission system based on orbital angular momentum beam multiplexing employing optical frequency comb. *Optical and Quantum Electronics, 54*, 132. http://doi.org/10.1007/s11082-021-03509-3

FSAN (2020). *Full-Service Access Network*. https://www.fsan.org/

Ghoniemy, S. (2018). *Enhanced time and wavelength division multiplexed passive optical network* (*TWDM-PON*) *for triple-play broadband service delivery in FTTx Networks* [Conference presentation]. 2018 International Conference on Computer and Applications (ICCA), Sydney, Australia.

Houtsma, V., Mahadevan, A., Kaneda, N. and Veen, D-V. (2021). Transceiver technologies for passive optical networks: Past, present, and future [Invited Tutorial]. *IEEE/OSA Journal of Optical Communications and Networking 13*(1), A44-A55. https://doi.org/10.1364/JOCN.403500

IEEE (2018). *IEEE Standard for Ethernet 802.3-2018* (*Revision of IEEE Std 802.3-2015*). https://doi.org/10.1109/IEESTD.2018.8457469

Jaramillo-Villegas J. A., Xue. X., Wang, P. H., Leaird, D. E., and Weiner, A. M. (2015). Deterministic single soliton generation and compression in microring resonators avoiding the chaotic region. *Optics Express 23*(8), 9618-9626. https://doi.org/10.1364/OE.23.009618

Jørgensen, A. A., Kong, D., Henriksen, M. R., Klejs, F., Ye, Z., Helgason, Ò. B., Hansen, H. E., Hu, H., Yankov, M., Forchhammer, S., Andrekson, P., Larsson, A., Karlsson, M., Schröder, J., Sasaki, Y., Aikawa, K., Thomsen, J. W., Morioka, T., Galili, M., Torres-Company, V., and Oxenløwe, L. K. (2022). Petabit-per-second data transmission using a chip-scale microcomb ring resonator source. *Nature Photonics, 16*(11), 798-802. http://doi.org/10.1038/s41566-022-01082-z

Komagata, K., Tusnin, A., Riemensberger, J., Churaev, M., Guo, H., Tikan, A., and Kippenberg, T. H. (2021). Dissipative Kerr solitons in a photonic dimer on both sides of exceptional point. *Communications Physics, 4*, 159. https://doi.org/10.1038/s42005-021-00661-w

Kippenberg, T. J., Gaeta, A. L., Lipson, M., and Gorodetsky, M. L. (2018). Dissipative Kerr solitons in optical microresonator. *Science, 361*(6402), 361-567. https://doi.org/10.1126/science.aan8083

Lundberg, L., Mazur, M., Mirani, A., Foo, B., Schröder, J., Torres-Company, V., Karlsson, M., and Andrekson, P. A. (2020). Phase-coherent lightwave communications with frequency combs. *Nature Comunications, 11*, 201. https://doi.org/org/10.1038/s41467-019-14010-7

Ma, W., Liu, Z., Kudyshev, Z. A., Boltasseva, A., Cai, W., and Liu, Y. (2021). Deep learning for the design of photonic structures. *Nature Photonics, 15*, 77-90. https://doi.org/10.1038/s41566-020-0685-y

Mittal, S., Moille, G., Srinivasan, K., Chembo Y. K., and Hafezi, M. (2021). Topological frequency combs and nested temporal solitons. *Nature Physics, 17*, 1169-1176. https://doi.org/10.1038/s41567-021-01302-3

Qi. Z., Wang, S., Jaramillo-Villegas J. A., Qi. M., Weiner, A. M., D'Aguanno G., Carruthers T. F., and Menyuk, C-R. (2019). Dissipative cnoidal waves (Turing rolls) and the soliton limit in microring resonators. *OSA Journal, 6*(9), 1220-1232. https://doi.org/10.1364/OPTICA.6.001220

Rodríguez-García, A. B., Ramírez-López, L., and Travieso-Torres, J. C. (2015). New heuristic algorithm for dynamic traffic in WDM optical networks. *Ingeniería e Investigación, 35*(3), 100-106. https://doi.org/10.15446/ing.investig.v35n3.51676

Serpa-Imbett, C. M., Gómez-Cardona N. D., Borrero. A., and González, N. (2009). Design and construction of a fiber optic network for analysis of topologies and transmission Design in devices for WDM-PON networks. *TecnoLógicas, 23*, 55-64. https://doi.org/10.22430/22565337.236

Shbair, W. W., El-Nahal, F. I. (2021). Coherent passive optical network for 5G and beyond transport. *Optoelectronics Letters, 17*, 546-551. https://doi.org/10.1007/s11801-021-0178-3

Thangappan, T., Therese, B., Suvarnamma, A., and Swapna, G. S. (2020). Review on dynamic bandwidth allocation of GPON and EPON. *Journal of Electronic Science and Technology, 18*(4), 100044. https://doi.org/10.1016/j.jnlest.2020.100044

Van Veen, D. (2020). *Transceiver technologies for next-generation PON* (*Tutorial*) [Conference presentation]. Optical Fiber Communication Conference and Exhibition (OFC), San Diego, CA, USA.

Xiaobao, Z., Hui, L., Wei, X., Xinlin. C., Xiang. H., and Guangzong, X. (2021). *Numerical study of dissipative Kerr soliton generation in a microcavity processed by sol-gel method* [Conference presentation]. First Optics Frontier Conference, Hangzhou, China.